Title

ABSOLUTE DIFFERENTIAL CROSS SECTION FOR PRODUCTION OF ENERGETIC 8-RAY ELECTRONS BY 1.12-Bev/c PIONS

Author

Crawford, Frank S.

Publication Date

1959-08-01

UCRL 8876

UNIVERSITY OF CALIFORNIA

Ernest O. Lawrence

Radiation Laboratory

BERKELEY, CALIFORNIA

DISCLAIMER

UCRL-8376

UNIVERSITY OF CALIFORNIA

Lawrence Radiation Laboratory
Berkeley, California

Contract No. W-7405-eng-48

ABSOLUTE DIFFERENTIAL CROSS SECTION FOR PRODUCTION OF ENERGETIC δ-RAY ELECTRONS BY 1.12-Bev/c PIONS

Frank S. Crawford, Jr.

August 1959

ABSOLUTE DIFFERENTIAL CROSS SECTION FOR PRODUCTION OF ENERGETIC δ-RAY ELECTRONS BY 1.12-Bev/c PIONS

Frank S. Crawford, Jr.

Lawrence Radiation Laboratory
University of California
Berkeley, California

August 1959

Abstract

We have measured the absolute differential cross section $d\sigma/dK$ for production of delta-ray electrons by 1.12-Bev/c negative pions incident on a 10-in. liquid hydrogen bubble chamber, for values of the δ-ray kinetic energy K between 32 Mev and the kinematical upper limit of 62 Mev. The results are in agreement with the theoretical prediction of Bhabha. We find an integrated cross section

$$\sigma(K > 32 \text{ Mev}) = 1.37 \pm 0.17 \text{ mb.}$$

This exceeds the theoretical prediction of 1.17 mb by a factor 1.17 ± 0.15.

The monoenergetic electron contamination of the pion beam has been determined by counting electron-induced δ rays. The monoenergetic and non-monoenergetic contributions to the muon contamination have both been determined by combining a determination of the number of muon-induced δ rays with a measurement of the curvature distribution of beam tracks. The method is described in detail.

ABSOLUTE DIFFERENTIAL CROSS SECTION FOR PRODUCTION OF ENERGETIC δ-RAY ELECTRONS BY 1.12-Bev/c PIONS*

Frank S. Crawford, Jr.

Lawrence Radiation Laboratory
University of California
Berkeley, California

August 1959

In the Berkeley experiment on associated production of strange particles by 1.12-Bev/c π^- incident on the Alvarez 10-inch hydrogen bubble chamber it was necessary to determine the electron and muon contamination present in the pion beam, in order to obtain absolute cross sections. The method used was to count energetic δ-ray electrons produced by beam particles. The identity of the beam particle in a δ-ray event is obtained from the electron energy and angle. The number of incident electrons and muons is obtained from the corresponding number of δ rays by using the theoretical production cross sections.[1,2,3] The cross section for δ-ray production by pions was measured, as a check on the over-all experimental method, as well as on the theoretical expression for the cross section. In this article we describe the measurement of the pion cross section and the determination of the electron and muon contamination of the pion beam.

---

*Work done under the auspices of the U. S. Atomic Energy Commission.

Kinematics

The laboratory-system (lab) angle θ and lab kinetic energy K of the struck electron are most concisely related through the center-of-mass-system (c.m.) angle θ_c of the electron, by

$$\tan\theta = (1/\bar{\gamma})\tan\theta_c/2, \quad \text{and} \tag{1}$$

$$K = 2m_e \bar{\eta}^2 \cos^2\theta_c/2. \tag{2}$$

Here m_e is the electron rest energy, 0.511 Mev; $\bar{\gamma}$ is $(1-\bar{\beta}^2)^{-1/2}$; $\bar{\eta}$ is $\bar{\gamma}\bar{\beta}$; and $\bar{\beta}$ is the velocity of the c.m. system with respect to the lab system. Elimination of θ_c from Eqs. (1) and (2) gives

$$K = 2m_e \bar{\eta}^2 \cos^2\theta/(1 + \bar{\eta}^2 \sin^2\theta). \tag{3}$$

The maximum electron kinetic energy K_m is given by

$$K_m = 2m_e \bar{\eta}^2. \tag{4}$$

The c.m. motion is given by

$$\bar{\eta}^2 = \eta^2 [1 + 2\gamma(m_e/m) + (m_e/m)^2]^{-1}. \tag{5}$$

where m is the rest energy of the incident particle, and where γ and η correspond to β, the lab velocity of the incident particle. The lab momentum of the incident particle is ηm. The electron velocity in the rest frame of the incident particle is $-\beta$.

We do not give the kinematics of the outgoing primary particle, since except for the case in which the incident particle is an electron the primary particle is not much affected, at incident momenta as low as 1 Bev/c. For instance, the maximum transverse momentum given to a 1.12-Bev/c pion is 4 Mev/c, corresponding to a deflection of only 0.2 degree.

For an incident particle of rest energy m Eq. (5) shows that the c.m. system is practically identical with the rest system of the incident particle,

as long as the target electron's total mass γm_e in that system is small compared with m, that is, as long as the total lab energy γm of the incident particle satisfies

$$\gamma m << m^2/m_e, \tag{6}$$

which is 22 Bev for incident muons, 38 Bev for pions, or 478 Bev for K mesons. For instance, at 1.12 Bev/c $\bar{\eta}$ is less than η by only about 3% for pions, or 4% for muons.

Equations (4) and (5) show that when (6) holds the energy K_m of a knock-on electron is approximately $2m_e\eta^2$, that is, $2m_e p^2/m^2$, for a given incident momentum p. Thus K_m goes inversely as the square of the rest mass m of the incident particle, for a momentum-selected beam, and knock-on electrons can provide a sensitive determination of m.[4,5] For example, a 1.12-Bev/c muon can produce a knock-on electron of kinetic energy 104 Mev, compare to a maximum of 62 Mev for a pion of the same momentum.

For relativistic incident particles ($\bar{\eta} >> 1$), Eq. (3) shows that for $\sin\theta >> 1/\bar{\eta}$, K is independent of the incident mass and momentum, and depends only on the lab angle θ. Therefore only the energetic electrons having $K >> K_m/2$ (i.e. $\sin\theta << 1/\bar{\eta}$) are expected to be useful.

The smooth curves in Fig. 1 summarize the kinematics of energetic δ-ray production by 1.12-Bev/c incident electrons, muons, pions, and K mesons.

Experimental Details

In the first scan of the film for associated production events δ rays were not recorded. About 26,000 frames taken at 1.12 Bev/c were rescanned for energetic δ rays. Figure 2 shows a 42-Mev pion-induced δ ray typical of those included in the determination of the pion cross section. Figure 3 shows the most energetic δ ray found. Its energy and lab angle are plotted as event "a" in Fig. 1, and are consistent with δ-ray formation by a 1.12-Bev/c electron.

Scanning was done along the projected image (~ 4/3 natural size) of each beam track. A "candidate" δ ray was recorded if its radius of curvature ρ projected on the scanning table was greater than 4.0 inches, and if the production point lay inside a fiducial area drawn on a template which could be aligned with fiducial marks in the chamber. The criterion $\rho > 4$ in. accepts all δ rays with more than 29 Mev/c and (because of the variation in magnification with vertical position in the chamber) some δ rays down to 23 Mev. The fiducial area had an average length of about 5.5 in. (natural size) in the beam direction and thus allowed about a 2-in. view of a beam track before it entered and after it left the fiducial area. The 2-in. exit space was used to insure measurability of the δ-ray curvature; the 2-in. entrance space was sufficient to determine whether or not it was a single beam track that entered the chamber, and thus provided a guarantee against accepting δ rays produced in the chamber wall.

The axis of the chamber, the direction of the magnetic field, and the axis of the optical system coincide. The stereo angle is rather small--the two lenses are 3.5 in. apart and are 46 in. above the median plane of the chamber. Also, the production angle of the δ rays accepted is always less than 7 degrees. For these reasons the projected radius of curvature is essentially the same in both stereo views. The "dip" correction to convert projected radius of curvature to three-dimensional curvature is therefore less than 1% and was not made. The momentum of the δ ray is obtained from the projected radius

of curvature, the known magnification, and the known magnetic field (about 11 kilogauss). A correction for ionization energy loss (about 2 Mev) is applied to find the δ-ray momentum at the point of production. Only δ rays with a kinetic energy K of at least 32 Mev at production are finally accepted.

For each candidate, the direction and curvature of the incident beam track are measured on the scanning table. To be acceptable, the beam track must lie within ± 3 deg to the average beam direction and have the correct radius of curvature (180 in., magnified). The beam-curvature criterion eliminates about 8% of the candidates, which are due to "resolvably curvy" (RC) low-momentum muons in the beam (discussed later).

It is clear from Fig. 1 that incident pions, muons, and electrons should be fairly easily distinguished by means of the δ-ray production angle and energy, for δ rays of more than about 55 Mev. At first, in order to increase the detectable yield of muon- and electron-induced δ rays, an attempt was made to measure δ-ray production angles to less than ± 1 deg so as to determine the identity of the incident particle for δ-ray energies as low as ~ 30 Mev. Measurements were accordingly made using the "Franckenstein" measuring projector and an IBM-650 kinematical reconstruction program. However, δ-ray events have several peculiarities that often make it difficult to determine the production angle with accuracy comparable to that obtainable in, for instance, an elastic π-p scattering, or an associated-production event. The deflection of the incident particle is very slight (less than 0.2 deg for a 1.12-Bev/c pion) and is therefore of no help in determining the point of interaction. For a "flat" δ ray the production angle can nevertheless be determined (see, for example, Figs. 2 and 3). But a steep δ ray is nearly superposed on the incident track in both views and the point of interaction is then difficult to determine -- a missing bubble (due to a statistical fluctuation) can easily lead to an error of several mm. But for a δ ray with $\rho = 4$ in. an error of 2 mm in the location of the interaction point gives a systematic shift of 1.1 deg in the δ-ray production angle.

For these reasons no attempt was made to measure δ-ray angles for δ rays of less than 55 Mev. Instead such δ rays were assumed in first order to be due to pions. Their number was then corrected at each δ-ray energy for the number of δ rays produced by the known electron and muon contamination of the beam, by use of the theoretical cross sections. This correction averaged about 8% at all δ-ray energies. The correction is calculated in the Appendix and appears as the small negative correction in the third column of Table I.

No second scanning was done for δ rays. However, in the same sample of film it was found (by second scanning) that single-vee associated-production events were found with an efficiency of 98 ± 1%. Delta-ray events appear to be at least as easy to find as single neutral vee events. Consequently a scanning efficiency of 98 ± 2% was arbitrarily assumed for finding δ rays.

In all frames containing "candidates," the number n of beam tracks inside the fiducial area was counted. Each beam track, by definition, lay within ± 3 deg of the average beam direction, and had the correct radius of curvature as determined on the scanning table by a curvature template, and did not undergo a nuclear interaction before crossing the center of the fiducial area. Candidate frames having 29 or more beam tracks inside the fiducial area were rejected. The average number $\bar{n}$ of beam tracks per picture was then obtained by the "linearly biased frames" track-counting method.[6] In this method, instead of averaging n over a random sample of pictures one averages 1/n over the "interesting" sample containing the candidates. The 1/n cancels the linear bias of the sample, and one obtains $1/\bar{n}$, where $\bar{n}$ is the desired expectation value of the average over a random sample. The result was $\bar{n} = 11.7 \pm 1.0$.

In each roll scanned the total number F of "good frames" having from 1 to 28 beam tracks was counted. From F, $\bar{n}$, and the average length $\bar{l}$ of a beam track we obtain the total path length L of beam particles in liquid hydrogen, $L = F\bar{n}\bar{l} = 172.4 \times 10^4$ inches. After correction for muon and electron

contamination (discussed later) this becomes 162.8×10^4 inches. At our bubble chamber operating conditions a 1-mb cross section corresponds to a mean free path of 1.125×10^4 inches, so that the above path length yields 144.7 ± 13.2 events per millibarn.

Pion Cross-Section Results

A total of 218 acceptable δ rays of more than 32 Mev kinetic energy was found. Of these, four (labeled a, b, c, and d in Fig. 1) are attributed to incident 1.12-Bev/c electrons, two (e and f, Fig. 1) to muons, and the remaining 212 to pions. Table I contains the pion-cross-section data. Figure 4 shows the experimental points. The smooth curve in Fig. 4 is a plot of the theoretical expression[2, 3] for the absolute differential cross section for δ-ray production by a particle of zero spin,

$$(d\sigma/dK)_{th} = (2\pi r_e^2 m_e/\beta^2 K^2)[1 - \beta^2(K/K_m)], \qquad (7)$$

with $K_m = 62.1$ Mev for a 1.12-Bev/c particle of pion rest mass.

Integration of Eq. (7) from K = 32 Mev to $K = K_m$ yields

$$\sigma_{th}(K > 32 \text{ Mev}) = 1.17 \text{ mb}. \qquad (8)$$

The experimental total cross section for production by pions of δ rays of more than 32 Mev is

$$\sigma_{exp}(K > 32 \text{ Mev}) = \frac{(212 - 17)/0.98}{144.7} = 1.37 \pm 0.17 \text{ mb}. \qquad (9)$$

The experimental result (9) exceeds the theoretical value (8) by a factor of 1.17 ± 0.15. Thus, within the statistics (1.2 std dev) the experimental results agree with the theory, both in magnitude and in dependence on K.

In principle, accurate determination of the δ-ray-production cross section can be used to explore directly the electromagnetic form factor of the pion. For 1.12-Bev/c pions the classical distance of closest approach in a knock-on collision of point particles is 0.4×10^{-13} cm, which is less than

one-third of $\hbar/m_\pi c$, the pion Compton wave length. However, one may not expect to see any large effect of the pion charge structure until the de Broglie wave length of the electron in the pion rest frame has decreased to about $\hbar/m_\pi c$, that is, until the electron momentum ηm_e in the pion rest frame has increased to about $m_\pi c$, or 140 Mev/c. This corresponds to a lab pion momentum ηm_π of m_π^2/m_e or 38 Bev/c. For 1.12-Bev/c pions, the electron momentum in the pion rest frame is only 4.1 Mev/c, and one does not expect to observe effects of pion structure. For instance, for a particle of pion mass and spin 1, the factor $[1 - \beta^2(K/K_m)]$ for spin-zero particles in Eq. (7) becomes[7, 3]

$$[1 - \beta^2(K/K_m)][1 + K(m_e/3m_\pi^2)] + [K^2/3\gamma^2 m_\pi^2][1 + K(m_e/2m_\pi^2)].$$

The latter factor (spin 1) differs by less than 1% from the former (spin-zero) for all K, for 1.12-Bev/c particles of pion rest mass. (For 6-Bev/c pions, the latter factor exceeds the former by about 8% over the interval $K/K_m = 0.8$ to 1.0, but the cross section, integrated over the same interval, is rather small--4.8 microbarn.)

Electron Contamination

The electron contamination of the beam presumably arises mostly from conversion in the 3-in. polyethylene target of decay γ rays from π^0 mesons produced in the target. These electrons have the same momentum distribution as the main π^- beam. Other electrons, mostly from π^0 production in the chamber walls, are usually distinguishable from beam tracks through their curvature or their direction, and are not considered here.

At δ-ray kinetic energies K greater than 62 Mev (the upper limit for production by 1.12-Bev/c pions), δ rays induced by electrons can be readily distinguished from pion- and muon-induced δ rays. The four most energetic δ rays indicated in Fig. 1 are attributed to incident electrons. The theoretical cross section[1,3] for δ-ray production by 1.12-Bev/c electrons is plotted in Fig. 5. Its integral from K = 62 Mev to $K = K_m = 560$ Mev is 4.0 mb. The path length, 172.4×10^4 in. of beam track, corresponds to 153.2 events per mb, so that the fraction f_e of electrons in the beam is given by

$$f_e = (4 \pm 2)/4 \times 153.2 = 0.0065 \pm 0.0033. \qquad (10)$$

Muon Contamination[8]

Figure 6 is a schematic representation of the geometry. The muon contamination arises primarily from three sources. (a) pion decays occurring near the target, (b) decays occurring between the target and the bending magnet, and (c) decays occurring beyond the bending magnet. Source (a) yields muons having the same momentum distribution as the pion beam--that is, an average value of 1.12 Bev/c, with an rms half-width of 8 Mev/c.[9]

We next consider source (b). Just before reaching the bending magnet, the beam of π's and μ's has a well-defined direction, because of the 36-in.-long 1/2-in.-wide collimator. After being deflected 30 deg and then traveling 250 in. from the bending magnet to the bubble chamber, the central ray of the beam is displaced about 125 in. A particle on the centerline but 4% low in momentum is displaced by an additional 6 in. and misses the chamber. Thus all muons present in the beam before the bending magnet is reached must have nearly the correct beam momentum in order to pass through the chamber. This conclusion still holds after taking into account the nonzero angular aperture of the collimator and the angular spread of the muons with respect to their pion parents. The fraction of the beam that is contaminated from sources (a) and (b)--that is, from muons that are nearly monoenergetic (ME)--is called f_{ME}, and is calculated after consideration of source (c).

About 10% of the pions that pass the center of the bending magnet decay between the bending magnet and the chamber. For a relativistic pion ($\beta = 1$), the lab momentum p_μ and lab angle θ_μ of the decay muon depend on the pion momentum p_π and muon decay angle θ_c in the pion rest system through the relations

$$p_\mu = p_\pi (0.787 + 0.213 \cos\theta_c) \qquad (11)$$

and

$$\gamma_\pi \tan\theta_\mu = \sin\theta_c/(3.685 + \cos\theta_c). \qquad (12)$$

The decay spectrum in θ_c is isotropic. Therefore the distribution in p_μ is flat over its range from 1.00 to 0.57 p_π. For a p_π of 1120 Mev/c we have $\gamma_\pi = 8.02$, so that the maximum muon lab angle θ_μ is 2.0 deg. For a decay occurring at the center of the bending magnet this corresponds to a maximum displacement of about 8 in. at the chamber. Thus a fair number of the muons born between the bending magnet and the chamber passes through the chamber.

Instead of attempting to calculate this contribution to the contamination, we measure it, taking into account the flatness of the distribution in p_μ. Figure 7 shows a curvature distribution of beam tracks. The radii of curvature ρ were determined on the scanning table by comparison with curvature templates. A square distribution in p_μ from 0.57 to 1.00 p_π corresponds in first order to a square distribution in ρ from ρ = 100 in. to 180 in. (magnified). The magnification is 15% less at the bottom of the chamber and 15% more at the top than the median value. This variation must be multiplied by the vertical beam distribution and then folded into the predicted square distribution. The scanner can easily resolve ρ = 140 in. from 180 in. but cannot resolve 160 in. from 180 in. The nonmonoenergetic muon contamination from source (c) is thus divided into a "resolvably curvy" (RC) part f_{RC} and an "unresolvably curvy" (UC) part f_{UC} in the ratio $f_{UC}/f_{RC} = (180 - 150)/(150 - 100) = 0.6$. Thus by measuring f_{RC} we at the same time determine f_{UC}. In the sample of film represented in Fig. 7 there are 39 RC tracks, and 734 tracks not resolvable from ρ = 180 in. The latter are of course mostly pions, but include the muon contamination f_{UC}. Thus we have $f_{RC}/(1 + 0.6 f_{RC}) = 39/734$, so that

$$f_{RC} = 0.056 \pm 0.012 \qquad (13)$$

and

$$f_{UC} = 0.6\, f_{RC} = 0.034 \pm 0.007. \qquad (14)$$

There are several checks on the method. In the first place, the distribution of the 39 RC tracks in Fig. 7 is in agreement with the expected

distribution. Next, the sum of f_{RC} and f_{UC} corresponds closely to 10%, the fraction of pions that decay after the bending magnet. Since the horizontal and vertical pion beam profiles at the chamber are somewhat larger than the corresponding dimensions of the acceptance volume in the chamber, it is true to first order that "as many muons decay into as out of" the orbits that pass through the chamber, so that $f_{RC} + f_{UC}$ is expected to include most of the decays. Finally, of the RC muons (0.57 to 0.83 of p_π), not all enter the chamber in the beam direction. This is not only because many of them decay at from 1 to 2 deg to the direction of their parent pion, but is also due to deflection in the fringe field of the bubble chamber magnet. The fringe field times path length integrates to about 10 kilogauss ft. This deflects the 1120-Mev/c pions through 4.0 deg between "minus infinity" and the entrance to the chamber. Muons having 0.57 p_π are deflected through 6.9 deg, and those with 0.83 p_π through 4.8 deg. Therefore the average direction of the RC muons should be shifted relative to the pion beam by 1.9 deg. The average measured direction of the 39 RC tracks of Fig. 7 is indeed found to be shifted, in the expected direction, by 1.8 ± 0.3 deg. This agreement shows, for instance, that very few of the RC tracks can be attributed to pion interactions in the bubble chamber entrance wall, since these would have the same (average) direction as the π beam.

Of the 39 RC tracks in Fig. 7, 10 would be rejected in a track count since they deviate by more than $\pm$ 3 deg from the average beam direction. (They are all included within $\pm$ 5 deg., as expected.) For making track-count corrections we therefore would use f'_{RC}, the part of f_{RC} satisfying the direction criterion, with

$$f'_{RC} = 0.04 \pm 0.007. \qquad (15)$$

Of course in a track count in which the curvature of each track is checked, the RC tracks are all rejected, and f'_{RC} is not used.

We must still determine f_{ME}, the monoenergetic (ME) contamination from decays occurring before the bending magnet. Here we make use of the muon-induced δ rays. We calculate the expected number of δ rays above 58 Mev produced by the already known nonmonoenergetic muon contamination f_{UC}, subtract this number from the observed number (two, see Fig. 1), and attribute the remainder to the contamination f_{ME}. Since the cross sections are known, this determines f_{ME}. A more detailed description follows.

The theoretical cross section for δ-ray production by monoenergetic muons is, at these energies, essentially the same as for production by pions, and is therefore given, with a suitably modified value of K_m and of β, by Eq. (7). The differential cross section for muons having 1.00 p_π, i.e. 1.12 Bev/c, is plotted in Fig. 5. To obtain the average cross section for f_{UC} we average Eq. (7) over a flat distribution in p_μ from 1.00 to 0.83 p_π, and then integrate from K = 58 to 104 Mev. The result is 0.18 mb. The path length in the δ-ray scan corresponds to 153.2 events per mb. The expected number of δ rays produced by the fraction f_{UC} is therefore $0.034 \times 153.2 \times 0.18 = 0.94 \pm 0.21$. Since this number does not exceed the observed number, two, we have no contradiction. By subtraction we then attribute $2 - 0.9$ or 1.1 ± 1.4 δ rays to f_{ME}. Since f_{ME} has the beam momentum p_π, we integrate Eq. (7), as plotted in Fig. (5) with K_m = 104 Mev, from K = 58 to 104 Mev, and obtain 0.48 mb as the cross section for f_{ME} to produce an observable δ ray. Combining the counts, path length, and cross section, we find

$$f_{ME} = 1.1/(153.2 \times 0.48) = 0.015 \pm 0.019. \qquad (16)$$

The electron and muon contaminations of the beam are thus completely determined. The only information used is that obtained from the bubble chamber pictures.

Acknowledgments

I am indebted to Dr. Luis W. Alvarez and Dr. Horace Taft for useful suggestions, and to Messrs. Vincent de Lany, Richard Fong, and Robert West for scanning assistance. The experiment was accomplished through the cooperation of the bubble chamber crew, under the direction of Messrs. Robert D. Watt and Glenn J. Eckman, and the Bevatron crew, under the direction of Edward J. Lofgren and Harry G. Heard.

Appendix

The small negative correction to the counts in column 3 of Table I is a correction for muon and electron contamination. As an example we calculate the correction for the first interval, at K = 34 Mev.

The total pion track length in liquid hydrogen corresponds to 144.7 counts per millibarn. For a contaminant fraction f, the correction ΔN is $f \times 144.7 \times (d\sigma/dK)\,\Delta K$, where ΔK is 4 Mev for the interval under consideration, and $d\sigma/dK$ is the cross section for the contaminant to produce a 34-Mev δ ray.

The electron contamination f_e is 0.0065. The electrons have the beam momentum. The cross section, from Fig. 5, is 0.22 mb/Mev at K = 34 Mev. Therefore ΔN_e is $0.0065 \times 144.7 \times 0.22 \times 4 = 0.83$. Similarly the monoenergetic component f_{ME} of the muon contamination contributes $\Delta N = 0.015 \times 144.7 \times 0.13 \times 4 = 1.13$ counts.

The "unresolvably curvy" (UC) component of the muon contamination has a flat distribution in p_μ from 0.83 to 1.00 p_π, corresponding to radii of curvature from 150 in. to 180 in. in Fig. 7. For $p_\mu = p_\pi$ we have K_m = 104 Mev; for 0.83 p_π, K_m is 73 Mev. Averaging Eq. (7) over p_μ from 0.83 to 1.00 p_π yields an effective K_m of 87.4 Mev and a cross section $d\sigma/dK = (255/K^2)(1 - K/87.4)$ mb/Mev, which is 0.13 mb at K = 34. We therefore find $\Delta N = 0.034 \times 144.7 \times .13 \times 4 = 2.56$. The total correction is $\Delta N = 0.83 + 1.13 + 2.56 = 4.52$ counts to be subtracted from the 62 observed counts.

References

1. C. Møller, Ann. Physik 14, 531 (1932) calculates scattering of e^- on e^-. See also Ref. 3.

2. H. I. Bhabha, Proc. Roy. Soc. (London) A 164, 257 (1938), calculates scattering of particles of spin 1/2 (i.e., muons) and of spin zero (i.e., pions) on e^-. See also Ref. 3.

3. Theoretical expressions for production of delta-ray electrons by various incident particles are summarized by B. Rossi, High-Energy Particles (Prentice-Hall, Incorporated, New York, 1952), p 15 ff.

4. See for instance L. Leprince Ringuet and M. Lheritier, Compt. rend. 219, 618 (1944), for the earliest example of a K^+ mass determination, via a knock-on electron in a magnetic cloud chamber. I am grateful to Prof. L. W. Alvarez for calling this event to my attention, and for pointing out to me the usefulness of δ rays.

5. The method breaks down for extremely relativistic particles having total energy $\gamma m \gg m^2/m_e$, since then the term $2\gamma m_e/m$ dominates the denominator in Eq. (5), and K_m goes essentially to ηm, the incident momentum, independently of the value of m. This happens when the momentum in the c.m. system becomes much larger than either of the two rest masses, so that the two values of total mass become essentially equal. The two particles are then no longer distinguishable in the c.m. by their inertia.

6. F. Crawford, "The Method of Linearly-Biased Track Counting in Cross Section Determinations", Rev. Sci. Instr. (to be published).

7. H. J. Massey and H. C. Corben, Proc. Cambridge Phil. Soc. 35, 463 (1939).

8. For other methods of determining muon contamination, using counter techniques, see, for example, Cool, Piccioni, and Clark, Phys. Rev. 103, 1082 (1956).

9. Crawford, Cresti, Good, Stevenson, and Ticho, Phys. Rev. Lett. 2, 112 (1959).

Table I

Pion cross-section data. K is the electron average kinetic energy in the interval ΔK. N is the observed number of counts in ΔK, minus a correction for the contribution of electron and muon contamination in the beam. $(d\sigma/dK)_{th}$ is the theoretical cross section, Eq. (7). The over-all χ^2 is 12.4, with 6 degrees of freedom.

K (Mev)	ΔK (Mev)	N counts	$(d\sigma/dK)_{exp}$ (mb/Mev)	$(d\sigma/dK)_{th}$ (mb/Mev)	$\Delta\chi^2$
34.0	4.0	62 - 4.5	0.102±0.016	0.1010	0.00
38.0	4.0	37 - 3.5	0.059±0.012	0.0699	0.82
42.5	5.0	42 - 3.2	0.054±0.010	0.0458	0.67
47.5	5.0	34 - 2.3	0.045±0.0090	0.0277	3.69
52.5	5.0	26 - 1.8	0.034±0.0077	0.0153	5.96
58.5	7.0	11 - 1.7	0.0094±0.0038	0.0052	1.22
		212 -17.0			12.36

Figure Captions

Fig. 1. Kinematics of δ-ray production. δ-ray lab kinetic energy K is plotted versus δ-ray lab angle θ, for δ rays produced by 1.12-Bev/c incident e^-, μ^-, π^-, and K^-. The six experimental points (labeled a through f) correspond to the δ rays that were not consistent with production by incident pions. Events a, b, c, and d are attributed to incident electrons, e and f to muons. Frame numbers of these events are a, 233804; b, 319568; c, 229164; d, 254778; e, 252357; f, 248457.

Fig. 2. Typical energetic δ ray produced by a 1.12 - Bev/c pion. The δ-ray kinetic energy is 42 Mev.

Fig. 3. The most energetic δ ray found, having a kinetic energy K of 134 Mev. The lab angle and energy of the δ ray are plotted as event a in Fig. 1, and are consistent with δ-ray formation by a 1.12 Bev/c electron.

Fig. 4. Differential cross section for δ-ray production by 1.12-Bev/c pions. K is the kinetic energy of the δ-ray electron. The experimental points correspond to the 4th column of Table I. The smooth curve corresponds to the theoretical prediction, Eq. (7), and to the 5th column of Table I. There is no relative normalization between the theoretical curve and the experimental points -- all quantities are absolute.

Fig. 5. Theoretical δ-ray production cross sections for 1.12-Bev/c incident e^-, μ^-, and π^-, plotted against δ-ray kinetic energy K.

Fig. 6. Schematic diagram of beam geometry. Dimensions along the beam are to scale, others are not. The 6-Bev proton beam p strikes a 4-in. polyethylene target T, produces 1.12-Bev/c negative particles at 0.0 deg, which are deflected through 30 deg in the Bevatron field, pass through a thin window W and a 36-in. -long 1/2-in. -wide collimator C, are deflected through 30 deg by a magnet B, and focused by a two-element quadrupole lens L, to an image at the bubble chamber BC.

Fig. 7. Curvature distribution of beam tracks. ρ is the projected radius of curvature in inches, as measured on the scanning table. The main beam at 1.12 Bev/c corresponds to ρ = 18 in. and contains 734 counts, indicated by the heavy arrow. The remaining 39 counts at smaller ρ are attributed to muons from pions that decay after passing the bending magnet.

FIG. 1

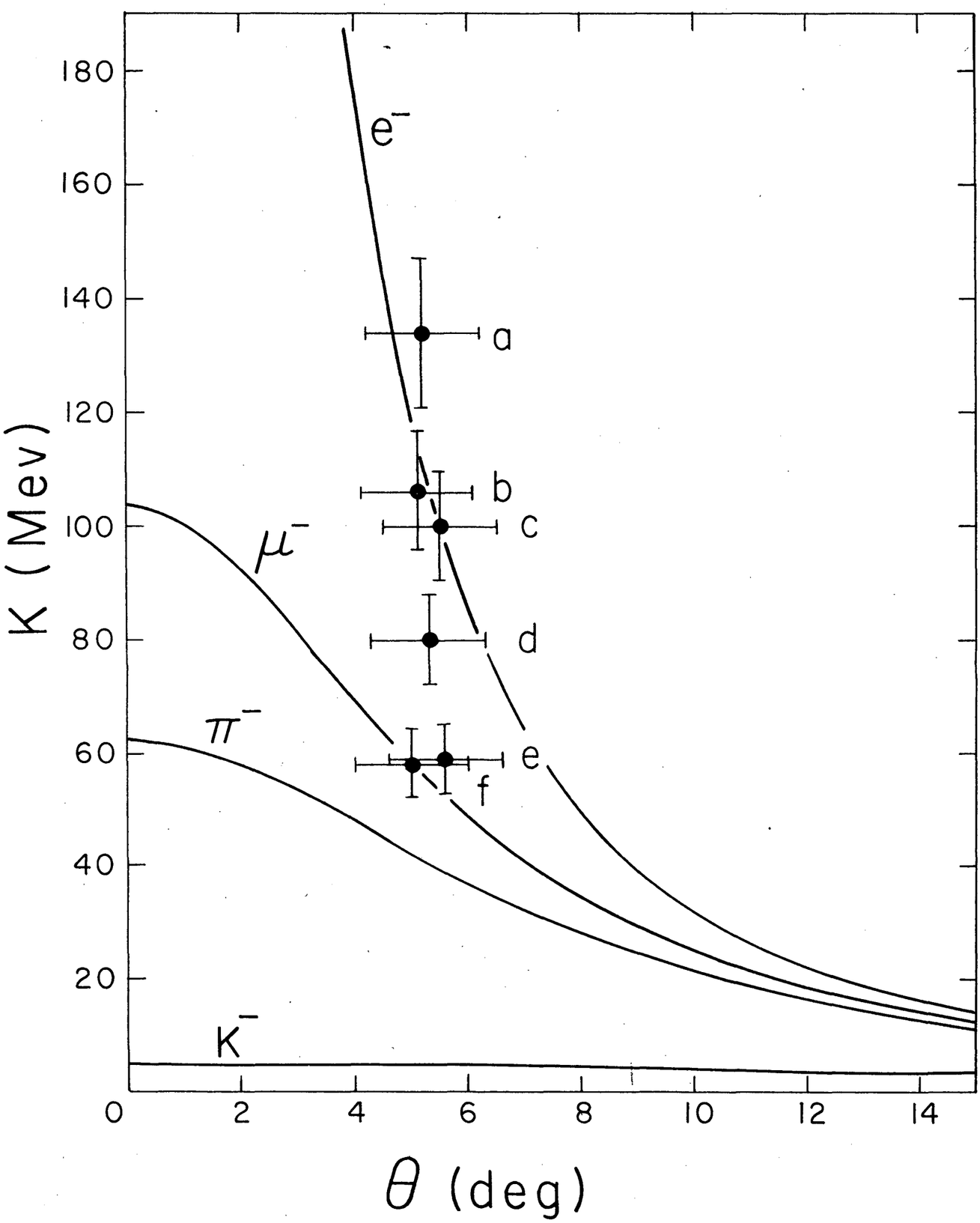
180
160
140
120
100
80
60
40
20
0
2
4
6
8
10
12
14
K (Mev)
θ (deg)
e⁻
μ⁻
π⁻
K⁻
a
b
c
d
e
f

Fig. 2

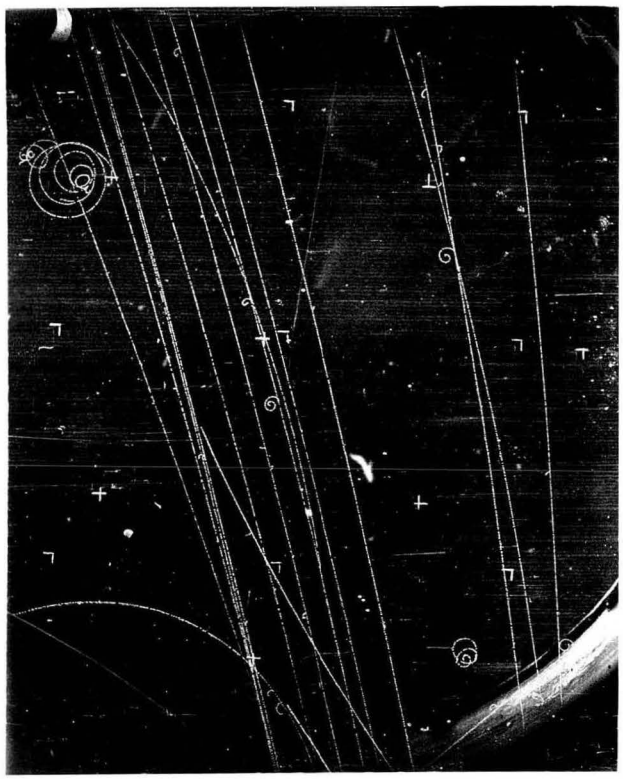

Fig. 3

FIG. 4

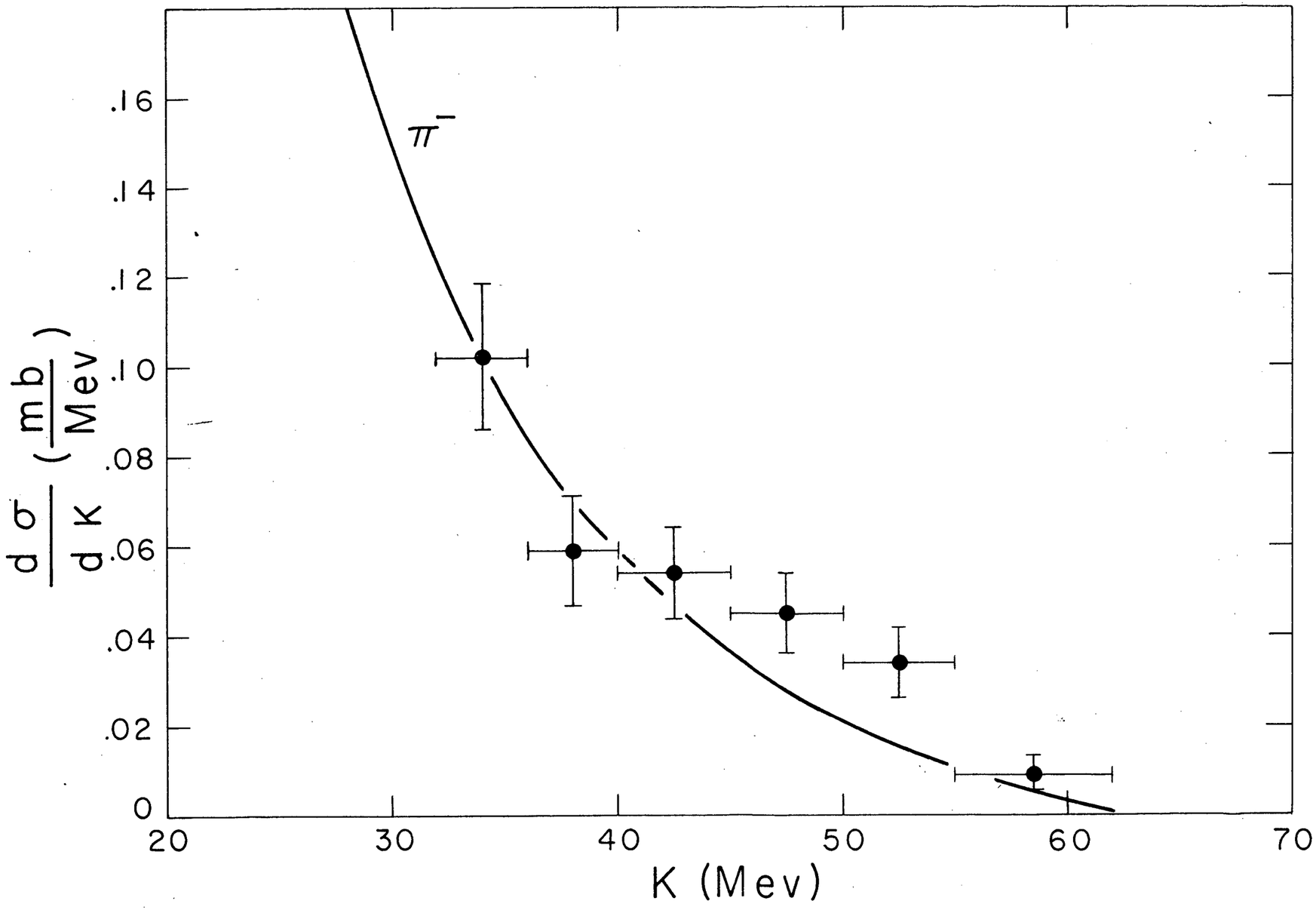
π^-
.16
.14
.12
.10
.08
.06
.04
.02
0
$\frac{d\sigma}{dK}$ ($\frac{mb}{Mev}$)
20
30
40
50
60
70
K (Mev)

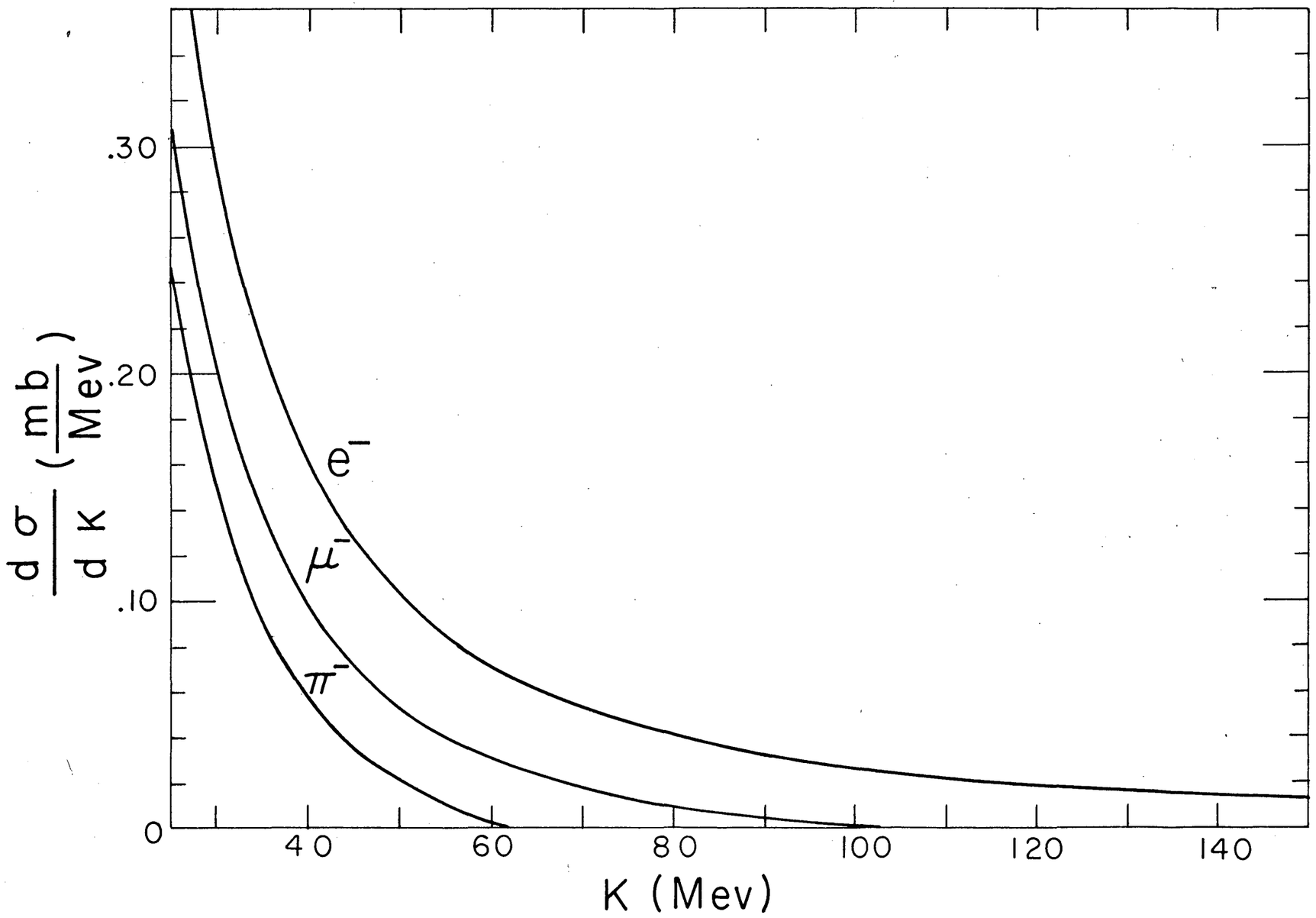
.30
.20
.10
0
40
60
80
100
120
140
K (Mev)
$\frac{d\sigma}{dK}$ ($\frac{mb}{Mev}$)
e^-
μ^-
π^-

FIG. 5

FIG. 6.

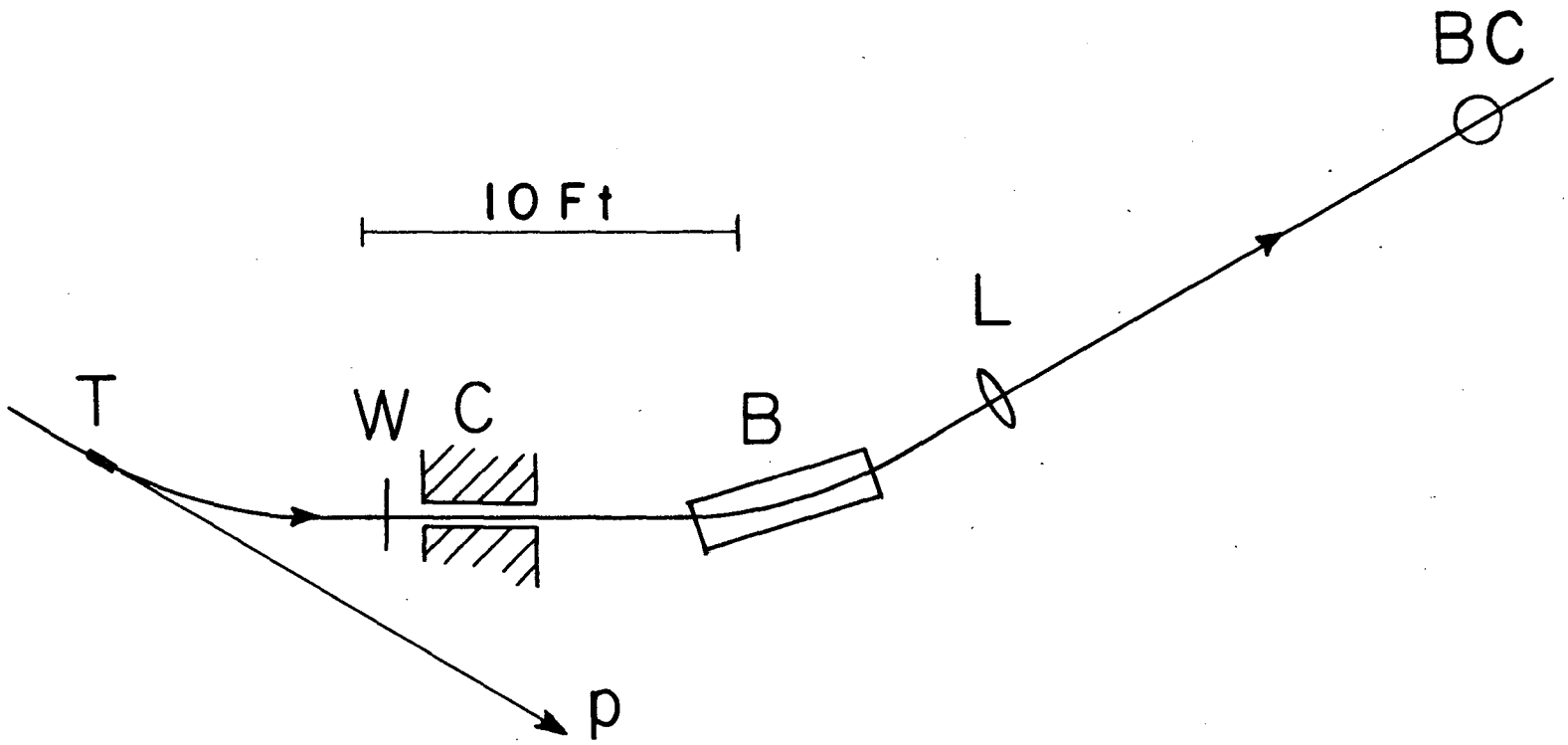

FIG. 7